

---

## “SPOP”(Specific Product Oriented Precipitation): A new concept to recover metals from mining waste water avoiding hydroxide sludge?

John, M. and Heuss-Aßbichler, S.

*Ludwig-Maximilians-Universität München, Theresienstr. 41, 80333 München, Germany,  
melanie.john@min.uni-muenchen.de*

**Abstract** Environmental pollution is a non-negligible issue for most mines and becomes an urgent task when acidic and metal loaded waters are created. “SPOP” is an environmentally friendly low-energy concept to protect water as a resource: the purified water can either be reused in various processing steps or discharged without environmental impact. The solid residues consist of precipitated oxides and native metals. This makes SPOP to a powerful method for secondary mining due to the economically attractive recovery of metals dissolved in aqueous solutions.

**Key words** water purification, metal recovery, secondary mining

### Introduction

Water pollution in mining industry is caused by acid mine drainage (AMD), effluents after mineral processing and from mill tailings as well as seepage from the impoundments. There are plenty of different physical, chemical or biological methods to treat metal (M) loaded mining waste water. They are categorized in active and passive treatment technologies, as for example membrane technology, and hydroxide precipitation using lime (e.g. Johnson & Hallberg 2005, Sheoran & Sheoran 2006, Simate & Ndlovu 2014). However, all state-of-the-art-techniques have well-known problems: For example, there is almost no membrane without fouling and what to do with the metal-bearing, partially toxic and highly voluminous hydroxide sludges? In general, these treatment technologies effect new waste streams (Simate & Ndlovu 2014). As for instance, dewatering of the secondary waste is costly and their deposit may harm the environment (Rakotonimaro et al. 2017). The potential of the metal resources hidden in mining waste water are mostly neglected (Gutiérrez et al. 2016, Rakotonimaro et al. 2017). Furthermore, water use is a critical issue in mining sites, in particular in arid climate zones. Hence, possible strategies for recovery of metals and water is becoming a more acute development task (Simate & Ndlovu, 2014, Nguyen et al. 2017).

“SPOP”: A procedure to recover transition and noble metals from industrial waste water

During the last years our research group worked on an innovative procedure to generate hydroxide free residues from different metal loaded aqueous solutions, called “SPOP” (Specific Product Oriented Precipitation). The basic principle of our method implies the presence or addition of variable amounts of  $\text{Fe}^{2+}$  ions to a metal loaded solution and subsequent alkalization with focus on prevention of voluminous hydroxides. The achieved recovery rates are very high, with  $\geq 99.99\%$  for Cu, Ni, Fe, Zn, Cr, Ag, Au and Mn. After treatment, the metal concentrations in waste water are in compliance with the limit values for direct dischargers in Germany.

All residues consist exclusively of M-Oxides, M-Fe-Oxides or metallic phases ( $M^0$ ). The composition of the residues is controlled by the reaction conditions (e.g. temperature, pH, redox state, kinetics) and in some cases ageing procedures. By optimizing these parameters, it is possible to gain directly from metal loaded waste water M-Oxides as ZnO, CuO,  $Cu_2O$  (Heuss-Aßbichler et al. 2016a+b, John 2016, John et al. 2016a+b), delafossite as  $CuFeO_2$ ,  $CuFe_{1-x}Mn_xO_2$  or  $AgFeO_2$  (John et al. 2016c, John 2016), M-ferrite, composite nanoparticles consisting of magnetite ( $Fe_3O_4$ ), M-ferrite ( $M_xFe_{3-x}O_4$ ) and delafossite ( $MFeO_2$ ) or pure zero-valent metals  $M^0$ , e.g. as foils ( $Ag^0$ ), or as nm to  $\mu m$  sized powders ( $Cu^0$ ,  $Au^0$ ) (Heuss-Aßbichler et al. 2016b, John 2016, John et al. 2016a). Our results clearly show that organic components or chelating agents, commonly present in industrial waste water do not harm the process. Due to the low volume and high metal content of the residues, the method can be an economic alternative for metalworking industries and helps to avoid dissipation of precious elements (Huber et al. 2016). Currently, a mobile pilot plant station (100l/h throughput) is constructed with the aim to upscale the laboratory experiments.

“SPOP”: A suitable concept to treat mining waste water?

Our method was originally developed and successfully tested to purify waste water from metalworking industries (Heuss-Aßbichler et al. 2016a, John 2016, John et al. 2016a-c). It combines efficient water purification with effective recovery of metals. Now, we adapted “SPOP” to treat mining waste waters. Our first results on synthetic mining waste waters at lab-scale are promising.

### Experimental setup and methods

The experimental setup contains of a reaction vessel (volume: 500 ml) which is equipped with a valve and a filter on the bottom of it. Both, valve and filter can be operated separately. First, the waste water was heated up to its natural elevated temperature (40 and 45 °C) using a heating plate and controlled by a thermocouple. Next, the solution was alkalized with NaOH. During this period the valve and the filter on the bottom of the vessel was kept closed. Once pH 8.5 was reached, the valve was opened to pass the purified waste water through the filter media. In the meanwhile NaOH was further added to achieve a pH between 9 and 10 for further 5 minutes in the reaction vessel. The pH was kept constant for at least 5 minutes. A fresh aliquot was taken, and the residual precipitates were aged 24 h under humid conditions. Afterwards, the precipitates were washed with water ( $\mu S/cm$ ) to remove the remaining co-precipitated salts and then dried at room temperature.

All residues are analysed using XRD and FTIR. Additionally samples were analysed using SEM, TEM and magnetic measurements (VFTB). Phase identification was performed by X-ray powder diffraction using a GE diffractometer 3003 TT. Samples were measured using  $Cu K\alpha_1$  radiation on a zero-background quartz holder. To gain better counting statistics, the holder was rotated during data collection. Each sample were measured 3 times at  $0.013^\circ$   $2\theta$  steps for an exposure time of 100 sec/count and summed to increase the signal/noise ratio. FTIR was applied to identify phases with low crystallinity. Therefore, an EQUINOX55 spectrometer from Bruker was used. The measuring conditions were: 64 scans, from  $360 -$

4000 cm<sup>-1</sup> with a scan time of 4 sec. All SEM images were taken with the NanoSAM Lab from Scienta Omicron at 10kV beam energy, a beam current of 100 pA, and a working distance of 5mm with an in-lens detector. Transmission electron microscopy (TEM) were carried out using a JEOL JEM-2100F. Magnetic responses to an applied magnetic field between -900 mT and +900 mT were analysed on a variable field translation balance (VFTB) from Petersen Analytics. All waste waters were measured with ICP-MS for Zn, Cu, Cd, Pb, As in accordance with DIN EN ISO 17294-2 and with ICP-OES for Fe in accordance with DIN EN ISO 11885.

### Material and sample series

The Richmond Mine of the Iron Mountain was the largest copper deposit in California, and it was mined until later 1940s for gold, silver, copper and zinc. The ore minerals occurred within massive sulphide lenses with 95% pyrite, variable amounts of chalcopyrite and sphalerite, and about 1% Cu and about 2% Zn. A large gossan was exposed near the surface of the weathered sulphide deposit causing a secondary enrichment up to 5–10% Cu and about 1 oz/yton Ag (Nordstrom et al. 2000). After underground renovations in 1990 extremely acidic mine water with pH values as low as -3.6 was observed and the amount of total dissolved solids was up to 900 g/L very high (Nordstrom & Alpers 1999). Acidic ferrous sulfate solutions caused by pyrite sulfide oxidation coupled with periods of intense evaporation of metal-rich acid mine water caused the precipitation of soluble, efflorescent salts (e.g. zincian-cuprian melanterite, rhomboclase and coquimbite) coating the surfaces of waste rocks, tailings and mine surfaces in underground and open pit area (Nordstrom & Alpers 1999). Table 1 summarizes typical temperatures, pH and chemical composition of mining waste waters found in the Richmond Mine of the Iron Mountain (Nordstrom et al. 2000).

**Table 1** Temperature, pH and chemical composition of mining waste waters found in the Richmond Mine, Iron Mountain, CA during September 1990 [Nordstrom & Alpers 1999].

Sample code	90WA101	90WA107
pH	1.51	0.46
T (°C)	40.6	47.1
SO <sub>4</sub> (g/L)	14	130
Fe (total) (g/L)	2.67	20.6
Fe (II) (g/L)	2.47	18.8
Zn (g/L)	0.058	2.28
Cu (g/L)	0.293	0.209
Cd (g/L)	0.0004	0.018
Pb (g/L)	0.0001	0.0042

Sample code	90WA101	90WA107
As (g/L)	0.003	0.046

Based on the water composition of Richmond Mine (see Tab. 1) we prepared two synthetic mining waste water (samples 101 and 107) using mainly highly soluble, hydrated sulfate salts. The pH was adjusted using concentrated  $H_2SO_4$ . Additionally we produced waste water with simplified compositions in order to identify those elements potentially problematic for the process. The chemical composition of the four synthetic waste water (samples 107\_sim\_a/b/c/d) shows Tab. 2.

**Table 2** Chemical composition of synthetic mining waste waters 101 and 107 and samples with simplified (= \_sim\_) composition

Sample code	101	107	107_sim_a	107_sim_b	107_sim_c	107_sim_d
SO <sub>4</sub> (g/L)	14	130	130	130	130	130
Fe (total) (g/L)	2.67	20.6	20.6	20.6	-	-
Fe (II) (g/L)	2.47	18.8	18.8	18.8	0.01	0.01
Zn (g/L)	0.058	2.28	2.28	2.28	2.28	2.28
Cu (g/L)	0.293	0.209	0.209	0.209	0.209	-
Cd (g/L)	0.0004	0.018	0.018	-	-	-
Pb (g/L)	0.0001	0.0042	0.0042	-	-	-
As (g/L)	0.003	0.046	-	-	-	-

### First results:

#### Water purification:

First results of Fe-rich samples show high recovery rates of almost 100 % for Fe, Zn, Cu, Cd and Pb for the samples 101, 107, and 107\_sim\_a, 107\_sim\_b (Tab. 3). In comparison the recovery rate of As is lower (sample 102 > 96 %, sample 107 > 76 %). But the results of sample 101 and 107 also show that the presence of As in the solution does not disturb the precipitation of the transition elements. The samples 107\_sim\_c and 107\_sim\_d, which simulate mining water with low Fe content achieved recovery rates > 98 % for Zn. Cu was removed to almost 100 % from sample 107\_sim\_c.

In general, best recovery rates occurred at pH 10 for Fe-rich waste waters and pH 9 for mainly Zn- and Cu-rich waste waters. Using the observed temperature of the mining waters (between 40 and 47 °C) as reaction temperature achieved good results for all experiments. However, lower temperatures seem to be more advantageous, as in case of samples 107\_sim\_c and 107\_sim\_d, an increase of the temperature from 40 °C to 45 °C resulted in a worsened water purification rate over 4 %.

### Mineralogical characterisation of the precipitates:

All solid residues we gained during this first study on synthetic mining waters consist of oxides as main phases. Table 4 summarizes the observed phases by XRD (X, x) and FTIR (F, f). Capital letters mark main phases and small ones indicate minor contents. Figure 1 a.) presents the x-ray pattern of zincite (ZnO) observed for sample 107\_d, which is representative for samples we obtained from waters with low Fe-content. Zincite crystallizes in lens-shaped 100 to 300 nm large particles that tend to agglomerate to  $\mu\text{m}$ -sized clusters. A very small amount of co-precipitated wulfingite (ZnOH) was observed by FTIR.

**Table 3** Reaction conditions and best results after treatment of synthetic mining water and those with simplified (= \_sim\_) composition. Chemical composition were measured with ICP-MS and ICP-OES (Zn, Cu, Cd, Pb, As = DIN EN ISO 17294-2 and Fe = DIN EN ISO 11885, respectively).

Sample code	101	107	107_sim_a	107_sim_b	107_sim_c	107_sim_d
Reaction pH	10	10	10	10	9	9
End pH (purified water)	8.8	9	8.9	8.8	8.7	8.7
Reaction temperature (°C)	40	45	45	45	40	40
Fe (mg/L)	0.09	0.51	0.44	0.42	< 0.005	< 0.005
Zn (mg/L)	< 0.02	0.12	0.06	0.06	0.20	0.19
Cu (mg/L)	0.039	0.096	0.033	0.035	0.042	-
Cd (mg/L)	< 0.0002	0.0004	0.0004	-	-	-
Pb (mg/L)	< 0.002	0.004	<0.002	-	-	-
As (mg/L)	0.004	1.1	-	-	-	-

**Table 4** Summary of identified solid phases. Phases identified by XRD and by FTIR are marked with X and F, respectively. Capital letters indicate main phases and small letters minor contents. Note, possible traces of additional phases are in the range of the detection limit of XRD and FTIR.

Sample code	Ferrite	Green Rust	Ferrihydrite	Cuprite	Zincite	Wulfingite
101	X, F	f		f		
101_aged	X, F		f	f		
107	X, F	f			f	
107_aged	X, F				f	
107_sim_a	X, F	f			f	
107_sim_a_aged	X, F				f	
107_sim_b	X, F	f			f	
107_sim_b_aged	X, F				f	

Sample code	Ferrite	Green Rust	Ferrihydrite	Cuprite	Zincite	Wulfingite
107_sim_c/_aged					X, F	f
107_sim_d/_aged					X, F	f

The precipitates obtained from Fe-rich waters (samples 101, 107, 107\_sim\_a and 107\_sim\_b) are black to brownish colour independent of ageing time. All x-ray pattern exclusively show peaks assigned to ferrite (Fig. 1 c). All samples show medium to strong magnetic properties. A separation of the magnetic precipitates from the reaction solution proceeded within less than 20 seconds (sample 107). Figure 1 d.) shows a magnetization curve of the solids. The saturation magnetisation ( $M_s$ ) of all samples ranges between  $77 \text{ Am}^2/\text{kg}$  (sample 107) and  $59 \text{ Am}^2/\text{kg}$  (sample 101\_aged) at room temperature. Pure magnetite shows a  $M_s$  of  $92 \text{ Am}^2/\text{kg}$  (Ashcroft and Mermin 2005). In comparison, copper ferrite has a much lower value of  $25 \text{ Am}^2/\text{kg}$ . All samples show two different Curie temperatures ( $T_{c1}$  and  $T_{c2}$ ). The values of  $T_{c1}$  are  $230 \text{ }^\circ\text{C} - 265 \text{ }^\circ\text{C}$ , which may be assigned to zinkferrite (John 2016) and of  $T_{c2}$  are  $490^\circ\text{C} - 520 \text{ }^\circ\text{C}$ , indicating copper ferrite (Ashcroft and Mermin 2005). Both,  $M_s$  and  $T_c$  confirm an at least partial incorporation of Cu and Zn into the ferrite structure.

Using FTIR, we observed a main absorbance band assigned to magnetite. However, all samples show that the position of the characteristic band of magnetite at  $580 \text{ cm}^{-1}$  is slightly shifted to lower wave number ( $5$  to  $15 \text{ cm}^{-1}$ , see Fig. 1 e). We additionally identified in all samples the low-crystalline phase green rust by its characteristic absorbance bands at  $612$ ,  $668$ ,  $1102$ ,  $1144$  and  $3390 \text{ cm}^{-1}$  (see Fig. 1 e). During ageing, Green Rust transforms to ferrite. After 24 h the absorbance bands are hardly distinguishable from the background. Precipitates obtained from water 101 contain small amounts of Cuprite ( $\text{Cu}_2\text{O}$ ). During ageing a trace amount of ferrihydrite formed after 24 h. Figure 1 f.) shows a typical TEM image of nano-sized ferrites. Our results show that the ferrites usually agglomerate to larger clusters up to  $500 \text{ }\mu\text{m}$  large. Due to that, particle separation via filtration or magnetic approaches is facilitated. Even the co-precipitated tenardite ( $\text{Na}_2\text{SO}_4$ ), identified by its x-ray pattern (see Fig. 1 g), could be separated easily.

## Conclusions

SPOP was applied to purify acidic mine waste water polluted with various metals. After treatment, the water achieved high purification rates of nearly 100 %. The residues consist of oxides such as ferrite, cuprite and zincite. Thus, SPOP provides a sustainable solution to avoid new waste streams and presents an ecologically and economically method to recover metals from mine waste water.

## Acknowledgements

The authors would like to thank Dr. Aladin Ullrich of Universität Augsburg for performing SEM and TEM measurements, as well as Iphigenia Anagnostopoulos, Luisa Daxeder, Alicia Dorner and Kai Tandon for their assistance in sample preparation and measurement. We are grateful to Prof. Nikolai Petersen for his help at the VFTB, and Prof. Claudio Parica of Universidad Nacional de San Martin, Argentina, for helpful comment. This research was supported in part by the Bavarian State Ministry of the Environmental and Consumer Protection.

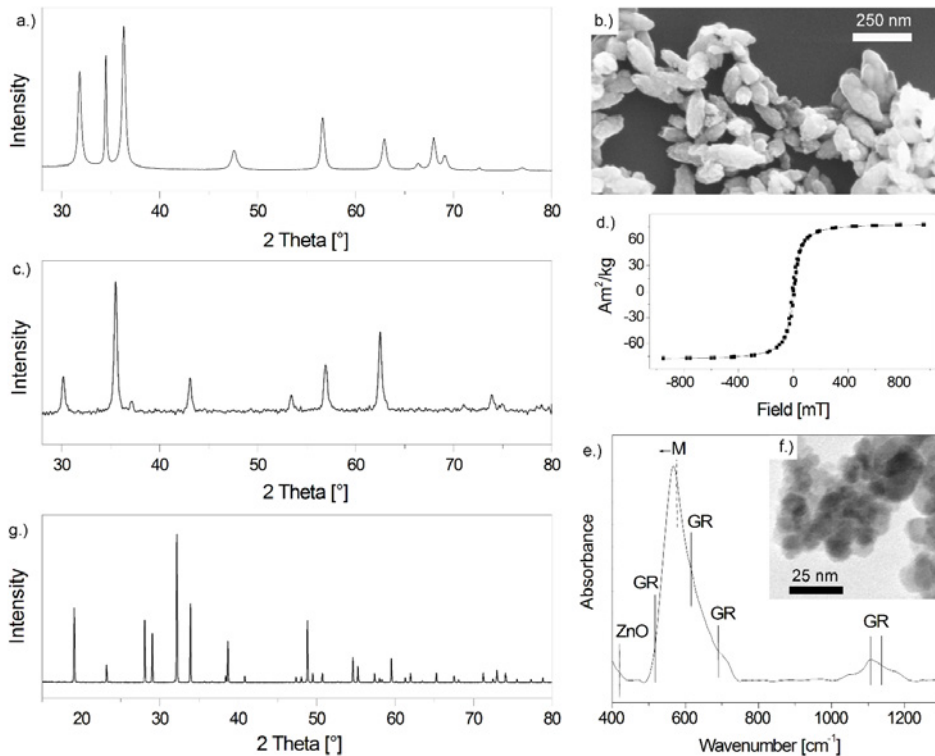


**Figure 1** XRD pattern (a.) and SEM image (b.) of zincite (ZnO in sample 107\_sim\_d. XRD pattern (c.) and hysteresis loop at room temperature (d.) of ferrite in sample 107. e.) FTIR spectrum of sample 107 showing green rust (GR) and zincite (ZnO). The most intensive absorbance band assigned to magnetite (M) is slightly shifted to lower wavenumbers. f.) TEM image of sample 107\_sim\_b showing nano-sized ferrites. g.) XRD pattern of co-precipitated salt (Na<sub>2</sub>SO<sub>4</sub>) of sample 107.

## References

- Ashcroft, N.W., Mermin, D.N. (2005) Festkörperphysik. Oldenburg Verlag.
- Gutiérrez M., Mickus K., Camacho L.M. (2016) Abandoned Pb Zn mining wastes and their mobility as proxy to toxicity: A review. Science of The Total Environment, 565: 392-400. doi.org/10.1016/j.scitotenv.2016.04.143
- Heuss-Aßbichler, S., John, M., Huber, A.L. (2016a) New procedure to recover heavy metals in industrial waste water. 8th International Conference on Waste Management and the Environment. WIT Transactions on Ecology and the Environment, 202: 85-96
- Heuss-Aßbichler, S., John, M., Klapper, D., Bläß, U.W., Kochetov, G. (2016b) Recovery of Cu as zero-valent phase and / or Cu oxide nanoparticles from waste water by ferritization. Journal of

Environmental Management 181: 1-7

- Huber, A.L., Heuss-Aßbichler, S., John, M. (2016) Is an effective recovery of heavy metals from industrial effluents feasible? in Pomberger, R. et al. (Ed.) 2016. *Abfallverwertungstechnik und Abfallwirtschaft* Eigenverlag / Montanuniversität Leoben, Leoben, Austria, p 721-724
- John, M. (2016) Low temperature synthesis of nano crystalline zero-valent phases and (doped) metal oxides as  $AxB_3-xO_4$  (ferrite),  $ABO_2$  (delafossite),  $A_2O$  and  $AO$ . A new process to treat industrial waste waters?
- John, M., Heuss-Aßbichler, S., Huber, A.L. (2016a) A new concept to recover heavy metals from industrial waste water. in Pomberger, R. et al. (Ed.) 2016. *Abfallverwertungstechnik und Abfallwirtschaft* Eigenverlag / Montanuniversität Leoben, Leoben, Austria, p 115-120
- John, M., Heuss-Aßbichler S., Ullrich, A. (2016b) Purification of waste water from zinc plating industry by precipitation of (doped) ZnO nanoparticles. *International Journal of Environmental Science and Technology*. 1735-1472
- John, M., Heuss-Aßbichler, S., Ullrich A, Rettenwander, D. (2016c) Purification of heavy metal loaded waste water from electroplating industry under synthesis of delafossite ( $ABO_2$ ) by “Lt-delafossite process”. *Water Research* 100, 98 – 104
- Johnson, D. B., & Hallberg, K. B. (2005) Acid mine drainage remediation options: a review. *Science of the total environment*, 338(1): 3-14.
- Nguyen, M.T., Vink, S., Ziemski, M., Barrett, D.J. (2014) Water and energy synergy and trade-off potentials in mine water management. *Journal of Cleaner Production*, 84, 629-638. doi.org/10.1016/j.jclepro.2014.01.063
- Nordstrom, D.K., Alpers, C.N. (1999) Negative pH, efflorescent mineralogy, and consequences for environmental restoration at the Iron Mountain Superfund site, California. *Proceedings of the National Academy of Sciences*, 96(7): 3455-3462.
- Nordstrom, D.K., Alpers, C.N., Ptacek, C.J., Blowes, D.W. (2000) Negative pH and extremely acidic mine waters from Iron Mountain, California. *Environmental Science & Technology*, 34(2), 254-258.
- Rakotonimaro, T.V., Neculita, C.M., Bussière, B., Benzaazoua, M., Zagury, G.J. (2017) Recovery and reuse of sludge from active and passive treatment of mine drainage-impacted waters: a review. *Environ Sci Pollut Res* 24(1): 73-91. doi:10.1007/s11356-016-7733-7
- Sheoran, A.S., Sheoran, V. (2006) Heavy metal removal mechanism of acid mine drainage in wetlands: a critical review. *Minerals engineering*, 19(2): 105-116. doi:10.1016/j.mineng.2005.08.006
- Simate, G.S., Ndlovu, S. (2014) Acid mine drainage: Challenges and opportunities. *Journal of Environmental Chemical Engineering*, 2(3): 1785-1803. doi.org/10.1016/j.jece.2014.07.021